

Basin-Scale Transmissivity and Storativity Estimation Using Hydraulic Tomography

by Kristopher L. Kuhlman¹, Andrew C. Hinnell², Phoolendra K. Mishra², and Tian-Chyi Jim Yeh^{2,3}

Abstract

While tomographic inversion has been successfully applied to laboratory- and field-scale tests, here we address the new issue of scale that arises when extending the method to a basin. Specifically, we apply the hydraulic tomography (HT) concept to jointly interpret four multiwell aquifer tests in a synthetic basin to illustrate the superiority of this approach to a more traditional Theis analysis of the same tests. Transmissivity and storativity are estimated for each element of a regional numerical model using the geostatistically based sequential successive linear estimator (SSLE) inverse solution method. We find that HT inversion is an effective strategy for incorporating data from potentially disparate aquifer tests into a basin-wide aquifer property estimate. The robustness of the SSLE algorithm is investigated by considering the effects of noisy observations, changing the variance of the true aquifer parameters, and supplying incorrect initial and boundary conditions to the inverse model. Ground water flow velocities and total confined storage are used as metrics to compare true and estimated parameter fields; they quantify the effectiveness of HT and SSLE compared to a Theis solution methodology. We discuss alternative software that can be used for implementing tomography inversion.

Introduction

Managing ground water resources requires knowledge of aquifer property distributions, since they affect water movement and solute transport. This understanding is often developed and tested with regional numerical ground water flow models, which are used for simulation, prediction, and scenario analysis. Regional models facilitate long-term management of water resources, where they can be used for both evaluation and mitigation of supply and quality issues.

In ground water model calibration, we seek to best represent a complex natural system with an idealized numerical model at the appropriate scale of interest. The

scale depends on the intended use of the calibrated model (e.g., flow vs. transport predictions) and the desired detail needed in the predictions. Many regional ground water studies do not attempt to build detailed heterogeneity into large-scale (tens to hundreds of kilometers) flow models, due to the prohibitive costs of detailed sampling over large areas and the computational limits on calibrating multiscale heterogeneity in the model. Regional geologic or hydrologic units are often treated as zones assumed to be homogeneous with a single effective parameter value (e.g., Barlebo et al. 2004). This zoned representation may offer computational advantages, but it can yield only large-scale effective properties, which are best for predicting “ensemble” behaviors of a ground water system (Yeh 1992; Yeh et al. 2007).

In regional studies that include local-scale heterogeneity (i.e., heterogeneity smaller than the hydrologic unit, at the scale of several model cells), the parameter distribution is often estimated from a steady-state or predevelopment head distribution (e.g., Yeh and Mock 1996). Heterogeneous transmissivity fields are estimated by manually adjusting parameter values in model cells or zones to match simulated and observed hydraulic heads. More advanced approaches use automated calibration algorithms (e.g., PEST [Doherty 2007] or UCODE [Poeter

¹Corresponding author: Department of Hydrology and Water Resources, University of Arizona, 1133 East James E. Rodgers Way, Tucson, AZ 85721; (520) 621-5082; fax: (520) 621-1422; kuhlman@hwr.arizona.edu.

²Department of Hydrology and Water Resources, University of Arizona, 1133 East James E. Rodgers Way, Tucson, AZ 85721.

³Department of Resources Engineering, National Cheng-Kung University, Tainan, Taiwan, R.O. China.

Received November 2007, accepted February 2008.

Copyright © 2008 The Author(s)

Journal compilation © 2008 National Ground Water Association.
doi: 10.1111/j.1745-6584.2008.00455.x

et al. 2005]) to minimize the residual between observed and simulated heads (Barlebo et al. 2004). Steady-state calibrations are limited to estimating transmissivity (T), and few regional studies attempt to calibrate ground water flow models using transient head measurements due to the large increase in complexity and computational effort.

Basin-scale transient model calibrations are often ill posed and nonunique due to difficulties collecting the necessary and sufficient information to make an inverse problem well posed (Yeh et al. 2007). As a result, there are many nonunique parameter distributions that equally fit sparse head observations. In other words, traditional inverse modeling efforts often yield ambiguous aquifer characterization. Because of the uncertainty inherent in aquifer parameter and boundary condition characterization, many modelers have developed misleading predictive models of ground water flow and contaminant migration. Because of this, some have seriously questioned the ability to validate ground water flow models at all (Konikow and Bredehoeft 1992; Oreskes et al. 1994; Bredehoeft 2003).

To improve our ability to adequately characterize and solve inverse ground water problems, we propose using hydraulic tomography (HT). Many researchers have shown that it can be used to characterize heterogeneous hydraulic properties, including Tosaka et al. (1993), Gottlieb and Dietrich (1995), Vasco et al. (2000), Yeh and Liu (2000), Bohling et al. (2002), Brauchler et al. (2003), and Zhu and Yeh (2005, 2006). HT involves collecting responses throughout an aquifer due to a sequence of overlapping aquifer tests and then calibrating a heterogeneous ground water flow model using the observed responses from all the tests. Multiple sets of aquifer tests and their observed responses improve the inverse problem, since tests cross validate each other. As a result, the estimated hydraulic property fields become more detailed and less uncertain than those computed from a single set of data.

HT has been applied successively to small-scale synthetic aquifers (Yeh and Liu 2000; Zhu and Yeh 2005, 2006; Hao et al. 2008), laboratory sandboxes (Liu et al. 2002, 2007; Illman et al. 2007), and plot-scale fields (Vesselinov et al. 2001; Bohling et al. 2007; Straface et al. 2007; Li et al. 2007). In these small-scale studies, it is possible to stress the entire domain with each pumping well, providing new information throughout the domain from each pumping event. We propose using regional-scale HT to estimate T and storativity (S) distributions for a regional flow model, where the main new challenge is determining how to adequately stress the entire aquifer. Unlike smaller-scale applications of HT, it is not possible to pump a single well causing a response throughout the aquifer; both the pumping rate and the test length would be unreasonably large. Realistically, a single aquifer test can stress only a portion of a large aquifer and cause measurable drawdown in only a subset of a basin-wide observation network. At the regional scale, we reformulate HT as an interference problem; the head distribution due to multiple simultaneous pumping wells is observed using a monitoring well network as might be found in a municipal water supply or remedial wellfield (off-duty pumping wells can serve as observation wells). Rather than successively pumping from

individual wells, we cycle through sets of pumping wells. In this way, the regional aquifer is repeatedly stressed to the fullest possible extent using existing wells.

We investigate the HT approach for estimating aquifer properties in a regional-scale ground water model; the method results in both more detailed (higher resolution) and more trustworthy (lower uncertainty) estimates. An improved estimate of aquifer properties is necessary to improve the reliability of predictions made with a calibrated model. Estimating aquifer parameters using the sequential successive linear estimator (SSLE; Zhu and Yeh 2005) with tomographic test data leads to better predictions of flow velocities and estimates of total storage for the basin, compared to traditional methods. The numerical analysis in this study was completed on a personal computer, demonstrating that HT inversion can be implemented using existing computer resources.

In this work, we use a synthetic regional confined aquifer to minimize unknown sources of error (e.g., measurement and model errors) that would complicate the analyses. Initially, we demonstrate that HT can be used on a regional scale and then we investigate the robustness of the method by changing the variance in the true field, adding random error to the head observations, and reducing the number of pumping events. Finally, HT was applied using observations of drawdown, rather than head, to investigate the effects of unknown initial and boundary conditions.

Methods

We solve the HT inverse problem using the SSLE algorithm, which is similar to that developed by Yeh and Liu (2000) and Zhu and Yeh (2005). The SSLE algorithm is an extension of the successive linear estimator that was developed for solving spatially variable parameter inverse problems using a geostatistical framework (Yeh et al. 1996; Zhang and Yeh 1997; Hughson and Yeh 2000). The implementation of the SSLE used here is coupled with the finite-element flow model VSAFT2 (Yeh et al. 1993) (available for free download at <http://www.hwr.arizona.edu/yeh>). We qualitatively discuss the key features of this approach; details on the SSLE are found in Zhu and Yeh (2005).

Because high-resolution parameter estimates are the desired result of tomographic inversion, we independently estimate parameter values (T and S) in each model element; this leads to a large number of free parameters. A successful tomographic approach applied at basin scale must overcome two hurdles. First, a large computational effort is required to estimate the sensitivity of model parameters to model predictions at observation locations. Second, additional constraints are needed to reduce the degrees of freedom in the solution, since there are more estimable parameters than calibration data (an ill-posed inverse problem).

The SSLE approach addresses both of these problems. First, the parameter-observation sensitivities required for the inverse problem are computed using the adjoint approach (Sykes et al. 1985; Sun and Yeh 1992), rather than using the perturbation approach (as in PEST or UCODE). The perturbation approach changes each

parameter independently, running the model forward to compute the corresponding model prediction change. With the perturbation inverse approach, a problem with 500 estimable parameters would require 501 (forward difference) or 1001 (central difference) independent forward model runs per iteration. For the adjoint approach, the effort to compute the model sensitivities is proportional to the number of observation data. This benefits problems with a large number of parameters and sparse observations, allowing sensitivities to be computed more efficiently. Second, due to the geostatistical foundation on which SSLE is built, the parameters being estimated (T and S) are not allowed to vary arbitrarily in space, but rather their distribution follows a geostatistical framework. Regularization (the observation that parameters vary “smoothly” in space [Tikhonov and Arsenin 1977]) is also a means of constraining the spatial distribution of parameters (implemented in PEST). The difference between the geostatistical and the regularization approaches is analogous to the distinction between kriging and inverse distance as interpolation schemes. Both kriging and SSLE incorporate additional geostatistical knowledge into their estimates, whereas Tikhonov-style regularization and inverse distance squared are purely empirical approaches. The geostatistical framework does have additional requirements (estimates of the mean, variance, and directionality of T and S), but the accuracy of these a priori estimates is not essential to the success of the algorithm in HT analyses (Yeh and Liu 2000).

Description of Synthetic Problem

The synthetic confined aquifer used here was designed to be realistically complex, while simple enough to allow straightforward interpretation of the results and the timely execution of many runs required for the robustness analysis. The two-dimensional (2D) model represents a depth-averaged heterogeneous 54×27 km aquifer, bounded by a river flowing west to east on the western, northern, and eastern boundaries and a mountain block on the southern boundary (Figure 1). The aquifer has two large bedrock outcrops, which are represented in the model by “islands”

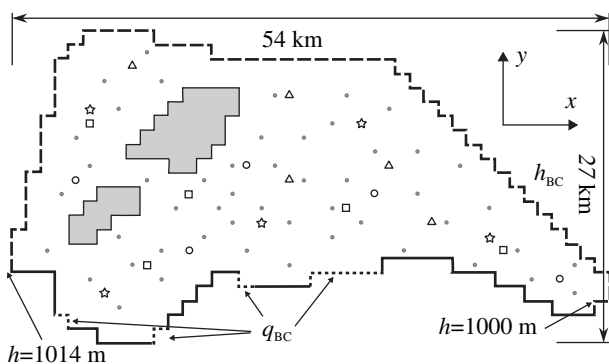


Figure 1. Map of domain showing pumping (open) and observation (solid) locations; Δ = event 1, \square = event 2, \star = event 3, and \circ = event 4. Dashed boundary is specified head, dotted boundary is specified non zero flux, and solid boundary is no-flow.

of no-flow cells (in Figure 1, inactive cells are gray). The finite-element mesh consists of 519 active square elements, each 1200 m on a side. The river is a specified head boundary condition, ranging linearly from 1015 to 1000 m from west to east (dashed boundaries in Figure 1). Specified flux boundary conditions (inflow) were used in four separate sections along the southern boundary to simulate fluxes into the model domain from neighboring basins (dotted boundaries in Figure 1).

A random true T field (Figure 2) was generated with an arithmetic mean of $300 \text{ m}^2/\text{d}$ and variance of $\ln(T)$ of 2.0, whereas the S field had an arithmetic mean of 0.001 and variance of $\ln(S)$ of 2.0. Transmissivity was assumed to be isotropic at the scale of the model elements ($T_x = T_y$), but both the T and the S fields were assumed to be statistically anisotropic at the scale of the domain. The correlation scale was 20 km in the east-west direction and 8 km in the north-south direction. The random T and S fields are uncorrelated; they used different random seeds during their generation. Initial conditions were the results of a steady-state simulation with no pumping.

HT was used to estimate the T and S fields by stressing the aquifer simultaneously with multiple pumping wells in a manner analogous to municipal pumping or a “pump-and-treat” remediation system. The synthetic wellfield comprised 70 wells: 20 pumping and 50 observation wells. All wells were located randomly within the domain using a Latin hypercube approach to limit spatial clustering. Although no specific effort was made to optimize the wellfield for aquifer parameter estimation, the subset of 20 pumping wells was visually selected to provide good spatial distribution of pumping wells throughout the synthetic aquifer. Pumping wells were assigned to one of four events such that each pumping event stressed most of

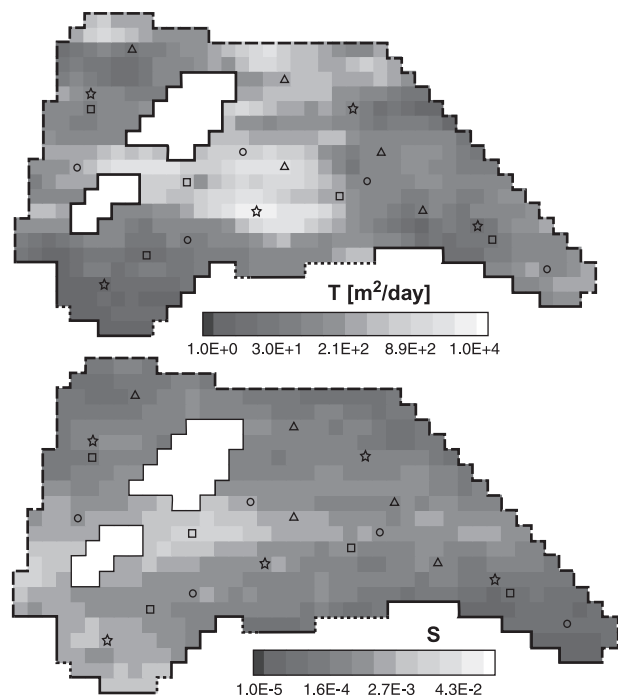


Figure 2. Map of true randomly generated T field with $\sigma_{\ln(T)}^2 = 2.0$ and mean = $300 \text{ m}^2/\text{d}$ and S field with $\sigma_{\ln(S)}^2 = 2$ and mean = 0.0001.

the aquifer, resulting in overlap between the stressed areas of different pumping events. The pumping well locations are shown as open symbols in Figure 1: triangles are wells pumped in pumping event 1, squares in event 2, stars in event 3, and circles in event 4. Each pumping event is an aquifer test that lasted 14 d, during which each of the five wells was pumped at 2000 m³/d (367 gallons per minute). The initial hydraulic head distribution for each pumping event was the steady-state head distribution. The aquifer response to each pumping event was observed at 50 observation wells (filled dots in Figure 1). For this example, we did not include the pumping wells from the other pumping events in the set of observation wells, although, in reality, one would include as many observation wells as possible.

Hydraulic head was sampled continuously at each observation well, but only four observation times from each pumping event were used in the inversion: three at early time and one at late time. These observation times were chosen to minimize the computational effort in the SSLE inversion while providing sufficient information to constrain the aquifer parameter estimates. For noise-free data, observations through time at one location are highly correlated, and each new temporal observation contributes little new information (Zhu and Yeh 2005).

The true and estimated parameter fields were compared using spatial distribution maps, scatter plots, and summary statistics. Good parameter estimates produce distributions that are visually “similar” and scatter plots with data clustered along the 1:1 diagonal. High correlation coefficient (ρ) indicates a significant linear relationship between the values of the two data sets, whereas high-rank correlation coefficient (ρ_{rank}) indicates that patterns of highs and lows are well correlated regardless of numerical values (Isaaks and Srivastava 1989). The L1 and L2 norms indicate the differences in the log mean (bias) and log standard deviation of the two data sets, respectively (Yeh and Liu 2000) (low norm values indicate better fit).

Quantitative comparisons were also made between the true and the predicted overall storage for the entire basin. When managing ground water basin resources, accurate information regarding the amount of water available from storage is essential. Last, we compared observed and simulated velocity fields (v_x and v_y), which are required in transport simulations. Whereas head is diffuse by nature and therefore easy to match, leading to nonunique solutions, solute transport is governed by advection (flow velocity, the gradient of head), which is much more sensitive to aquifer property distributions. Two head distributions can match observed point head measurements equally well but their corresponding flux distributions (and solute transport behaviors) may be very different. Velocity field comparisons provide a measure of how useful the simulation would be for making transport predictions.

Results

Estimation of T and S using Theis Solution

Aquifer parameters (T and S) are often estimated for real world applications using the Theis solution for

drawdown from a pumping well, even if some of its fundamental assumptions are known to be violated. The Theis solution is 2D (depth averaged) and assumes an infinite homogeneous aquifer. We modeled the drawdown observed during each pumping event using the Theis solution to both illustrate the inappropriateness of a homogeneous solution for interpreting heterogeneous regional-scale pumping tests and provide a comparison to the HT results.

We estimated T and S values from the “observed” model drawdown at observation wells. For simplicity, we assigned the estimated values to the location of the observation well, resulting in 50 estimates of T and S for each of the four pumping events. Drawdown at each observation well is due to pumping at five pumping wells. T and S are estimated by matching the observed drawdown to the drawdown predicted by summing the Theis solutions for the five pumping wells in a homogeneous infinite aquifer. PEST was used to minimize the sum of squared residuals between the observed and the Theis-simulated drawdown. The estimated parameter values at all 50 observation locations, for each pumping event, were then kriged to the flow simulation grid to generate the eight estimated parameter fields shown in Figures 3A and 3B. The eight model variograms used for kriging were derived by least-squares fitting an anisotropic exponential model to the experimental variograms created from the Theis results.

Due to the large domain, the simultaneous pumping of the five wells during each pumping period does not cause significant interference between the wells. The radius of influence of the pumping wells after 14 d of pumping (distance from the well to 1 cm of drawdown) varies between 4 and 15 km. However, more important for HT, at least 1 cm of drawdown was observed in 46/50 of the observation wells during at least two of the pumping events, and drawdown was observed in 26/50 of the observation wells for all of the pumping events.

We assigned parameters to observation locations rather than pumping locations because the latter would have resulted in 50 parameter estimates associated with 20 locations, requiring cokriging or additional averaging to be used in the flow model. T and S estimates could also have been attributed to a “representative” volume or location in the aquifer, but for heterogeneous aquifers, Theis-predicted values may change with time, orientation, and location (Wu et al. 2005). This makes interpretation of a representative location or volume difficult, especially with the presence of boundaries. Through the kriging of the intermediate point results onto the final flow simulation grid, we effectively volume averaged the Theis results in an objective and straightforward manner.

Visually comparing the Theis-estimated and true parameter fields (Figures 2 and 3), one can see that each pair of estimated T and S fields is different and a poor estimate of the true fields. As expected, the results of the Theis analysis are sensitive to boundaries. Although Li et al. (2007) indicate that Theis-based analyses can lead to estimates that agree, on average, with tomographic results, they did not have significant boundary conditions in their problem. The curve matching produced high values of T near the boundaries of the domain (Figure 3A),

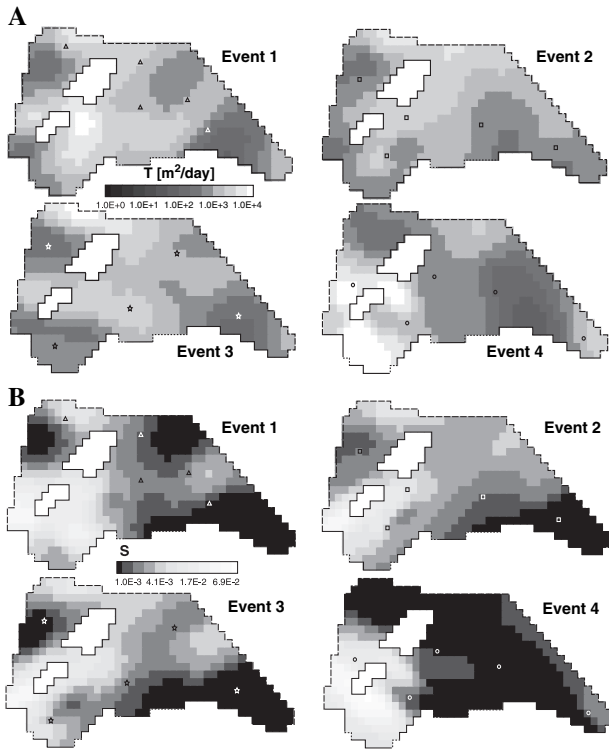


Figure 3. (A) Maps of estimated T using Theis analysis and (B) maps of estimated S using Theis analysis.

whereas high values of S were consistently predicted in the southwest corner of the domain (Figure 3B). The Theis analysis has produced four different distributions of T and S , which represent the head observations associated with the four pumping events. It is clear that the Theis solution does not give any useful information regarding the distribution of parameters (Li et al. 2007) because it is a homogeneous model. The hydrogeologist is left to average or decide which estimated parameter field they feel best represents the true field. More realistically, Theis analyses would be performed individually on each pumping test, potentially using distance drawdown to incorporate multiple observation wells at one time, but the hydrogeologist may be unaware that different overlapping tests can lead to markedly different results using a homogeneous model such as the Theis solution.

Although there are obvious limitations to using the Theis solution to analyze drawdown in a finite, heterogeneous domain, the exercise was done to illustrate two points. First, the results from the four pumping events, which used different pumping wells (but had many observation wells in common), do not produce identical or even similar results. This illustrates the fact that the Theis solution does not simply “average out” the heterogeneity around the pumping well (Wu et al. 2005). Although the shortcomings of the Theis solution are “obvious” in this synthetic example, it is a common practice to use Theis type curve analysis, with far less data, to analyze aquifer test results. In a real world case, unconfined, leakage, skin, wellbore storage, or partial penetration effects would also be compounded on the boundary and heterogeneity artifacts seen here. Here, these effects can

truly be ignored because the data are synthetic. The effects of ignoring wellbore storage or unconfined behavior may have a larger impact on predictions than the effects of ignoring distant boundary conditions, depending on field conditions.

Full Tomography Results

T and S fields were estimated using SSLE with error-free observations of head from 50 observation wells divided into the same four pumping events used in the Theis analysis. The estimated fields (Figure 4) compare favorably with the true fields (Figure 2). Scatter plots of the true and estimated parameters (Figure 5) show a low degree of bias (small L1 norm). Outlier parameter estimates are primarily located where the model is insensitive to parameter values: in cells adjacent to specified head boundaries and far from observation wells. The true and estimated T and S are well correlated (large ρ and ρ_{rank}). Summary statistics are listed for all the SSLE scenarios in Table 1 (panel a for T and panel b for S). Columns 1 to 4 give statistics for the base case, with no data noise and correctly specified boundary and initial conditions. Columns 5 and 6 show the effects of adding noise to observations and using the wrong boundary conditions (using all four pumping events). The last two columns give the statistics corresponding to the scenarios where the true random T and S fields were generated using the same random seed but different variances.

Since ground water velocity controls the advective transport of solutes, velocity fields were compared as a means to quantify the quality of the SSLE calibration. The x and y components of the velocity are well correlated with small L1 and L2 norms (Figure 6). The SSLE-estimated T and S fields would produce a reasonable estimate of advective solute transport, since accurate flow

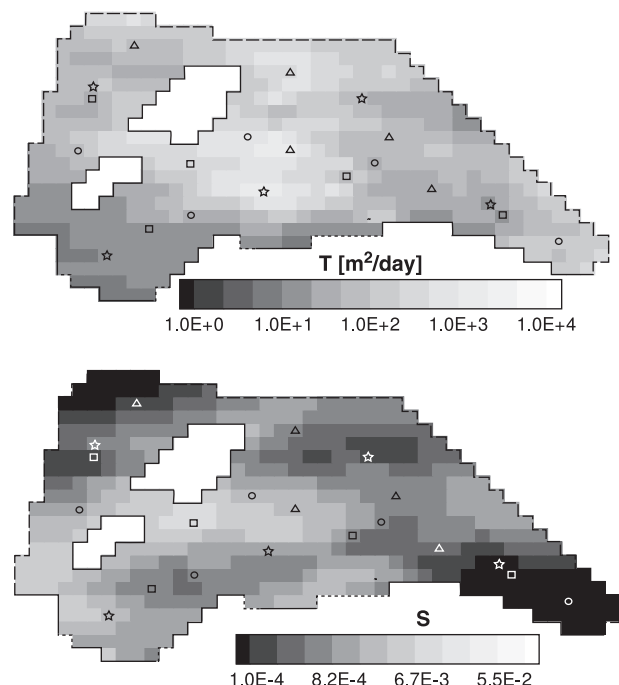


Figure 4. Maps of estimated T and S using SSLE method (all four pumping events).

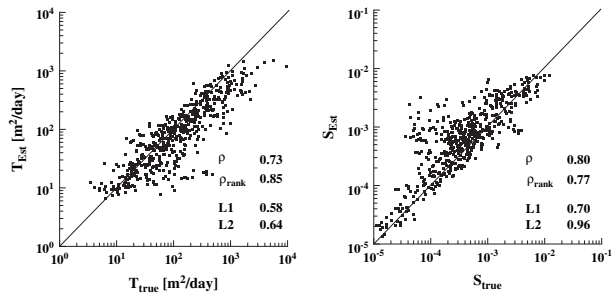


Figure 5. Scatter plots of estimated T and S using SSLE.

velocities are the most important part of a solute transport model.

Comparing the estimated and true total confined storage for the entire basin is another form of model validation. This quantity is found by summing the product of S and the area for each element, for all the elements in the domain. The area of all 519 model elements is $7.4736 \times 10^8 \text{ m}^2$, whereas the sum of the S (ΣS) in all elements is 0.4858 for the true field, giving a true total storage of $3.63 \times 10^8 \text{ m}^3$ (8225 acre-feet). The results of SSLE inversion gave $\Sigma S = 0.6425$ (overestimation by 32%), whereas the Theis approach gave $\Sigma S = 3.029, 2.302, 2.436,$ and 3.646 for events 1 through 4, respectively; the average Theis result is 2.853 (overestimation by 587%). Although SSLE does overestimate S , it is an order of magnitude better than the Theis solution. We interpret that because of the lack of boundary conditions in the Theis solution, it must overcompensate by overestimating the amount of water coming from aquifer storage. Overestimating available storage could easily lead to fallacious management decisions by basing long-term strategies on misinformation regarding available ground water.

Robustness Analysis

We tested the robustness of the HT inversion by changing several aspects of the synthetic example. First, we repeated the analysis with fewer pumping events, illustrating how HT leads to an improved estimate with additional information. Second, we added zero-mean Gaussian noise with a standard deviation of 0.1 m to the head data to better replicate field-measured observations. Third, the HT analysis was repeated with true T and S fields with variances of half ($\sigma_{\ln(T)}^2 = \sigma_{\ln(S)}^2 = 1$) and 1.5 times ($\sigma_{\ln(T)}^2 = \sigma_{\ln(S)}^2 = 3$) the levels of the original analysis. Finally, we reformulated the HT problem in terms of drawdown to minimize the effects of potentially unknown initial and boundary conditions.

Decreasing Number of Pumping Events

One of the main strengths of HT is the ability to use multiple data sets to estimate a single coherent parameter set. To illustrate the improvements from inverting multiple tests together, the analysis was repeated, each time removing more pumping events from the analysis. Inversion was performed using pumping events 1 through 3, 1 and 2, and pumping event 1 on its own. The scatter plots of true vs. estimated T and S for each analysis are presented in Figure 7, and the results from using all four pumping events are shown in Figure 4.

The T estimate improved as more pumping events (each with different pumping wells but the same observation locations) are inverted together. The cloud of points, representing T in each element of the flow model, moves closer to the 1:1 line as two and three pumping events are jointly inverted. This type of improvement is typical when inverting tomographic aquifer tests. Each pumping event adds new information to the overall estimate of the aquifer parameters, but no single pumping event by itself results in better parameter estimates than analyzing two

Table 1 Comparison of Summary T (Panel a) and S (Panel b) Statistics for Different SSLE Inverse Solutions								
(a) $\sigma_{\ln(T)}^2 = 2.0$								
	Event 1	Events 1–2	Events 1–3	Events 1–4	Noisy Observations	Drawdown + Incorrect Boundary Conditions	$\sigma_{\ln(T)}^2 = 1.0$	$\sigma_{\ln(T)}^2 = 3.0$
ρ	0.53	0.77	0.87	0.73	0.69	0.82	0.86	0.011
ρ_{rank}	0.77	0.86	0.89	0.85	0.82	0.84	0.93	0.033
L1	0.85	0.56	0.46	0.58	0.72	0.60	0.27	1.39
L2	1.25	0.58	0.42	0.64	0.89	0.87	0.13	2.90
(b) $\sigma_{\ln(S)}^2 = 2.0$								
	Event 1	Events 1–2	Events 1–3	Events 1–4	Noisy Observations	Drawdown + Incorrect Boundary Conditions	$\sigma_{\ln(S)}^2 = 1.0$	$\sigma_{\ln(S)}^2 = 3.0$
ρ	0.37	0.77	0.81	0.80	0.65	0.33	0.87	0.083
ρ_{rank}	0.67	0.73	0.74	0.77	0.76	0.71	0.87	0.031
L1	1.14	0.75	0.67	0.70	0.75	0.95	0.33	1.38
L2	2.20	1.13	1.01	0.96	1.05	1.46	0.22	3.07
Note: ρ and ρ_{rank} are the correlation and rank correlation coefficients. L1 and L2 are norms indicating bias and error in standard deviation, respectively.								

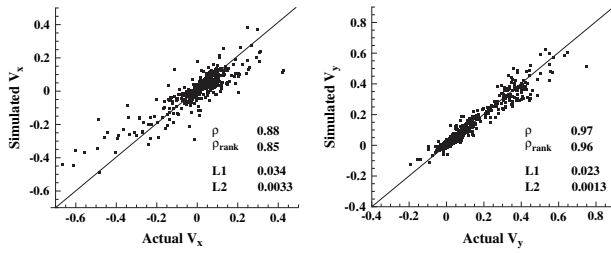


Figure 6. Scatter plots of x and y velocity components for SSLE-estimated T and S .

data sets simultaneously. The addition of each pumping event to the inversion process produces a smaller incremental improvement to the estimated parameters than the last addition, illustrating the diminishing returns of including similar data. Addition of a fourth pumping event noticeably decreases the quality of the estimated T field, whereas the quality of the estimated S field remains approximately the same, as can be seen in the summary statistics in Table 1. Using all four pumping events together may not produce optimal results for both parameters (in a nonsynthetic case, this would be difficult to quantify), but the SSLE results remain a very good estimate of the parameter distributions. In all scenarios, we used an SSLE convergence criterion of a 5% relative change in the estimated parameter variance.

Random Error Added to Observations

For the baseline analysis, the observations were noise free. In this case, we corrupted the data with unbiased Gaussian noise with a standard deviation of 0.1 m to

simulate more realistic observations. Corrupting the observations smooths the parameter estimates; however, the estimated parameter fields still generally agree with the true fields (Figure 8A), as can be seen by the high ρ_{rank} values. Corrupting the data effectively decreases the pumping well radius of influence (decreasing the signal to noise ratio), resulting in fewer observation wells with significant drawdown signal and increasing the scatter of the predicted flow velocities (Figure 8B). For the noisy data analysis, the same four observation times were used from each observation well and the same convergence criterion was used. This criterion aims at avoiding perfect fits between the observed and the simulated heads at the observation wells; this is useful when the observations are noisy.

The data can be smoothed before using them in the inversion process (e.g., with a moving average or wavelet smoothing), or the forward and inverse models will effectively do the smoothing, because the models cannot perfectly match noisy data. To improve the convergence of the inverse method, unexplained (especially biased) noise should be investigated and dealt with, if possible, to reduce its impact on the inverse solution (Xiang 2007).

Different Variances in True T and S Fields

In the previous cases, the true T and S fields were generated for a variance in $\ln(T)$ and $\ln(S)$ of 2. Here, we examine the effect of using a smaller and larger log variance ($\sigma_{\ln(T)}^2$ and $\sigma_{\ln(S)}^2$ of 1 and 3). Increasing the variance in the true field resulted in much poorer parameter estimates. Both ρ and ρ_{rank} are smaller and the norms and larger (columns 7 and 8 in panels a and b of Table 1). The

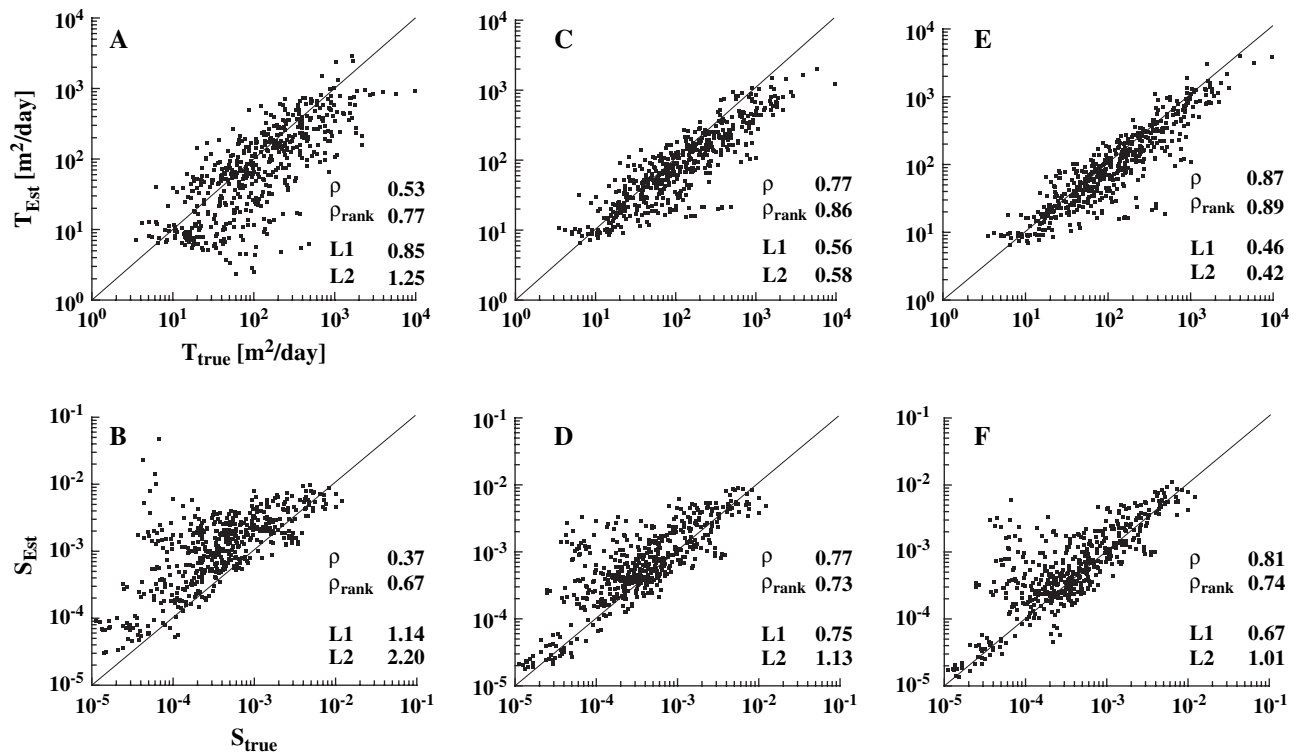


Figure 7. Scatter plots of SSLE inversion using different pumping events (top row is T , bottom row is S); A, B = event 1 only; C, D = events 1–2; and E, F = events 1–3 (see Figure 5 for events 1–4).

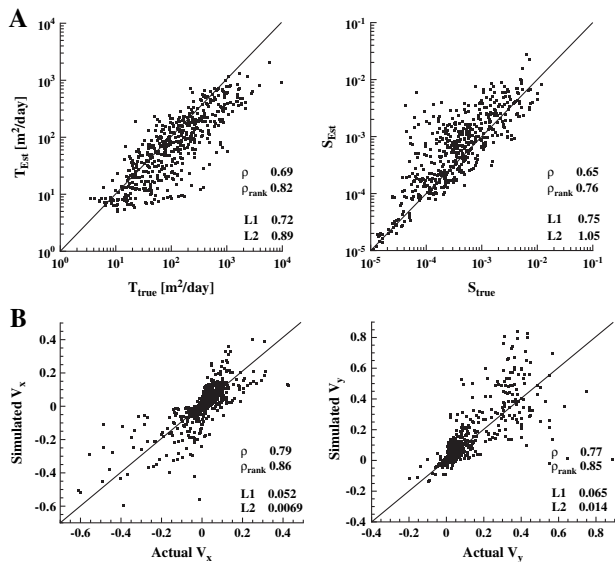


Figure 8. (A) Scatter plots of SSLE-estimated T and S with noisy ($\sigma = 0.1$ m) head observations and (B) scatter plots of x and y velocity components for SSLE-estimated T and S using noisy observations.

larger T and S parameter ranges associated with the larger variances are more difficult to estimate. As expected, the parameter estimates from the case with a lower variance are more accurately estimated (the true parameter fields are smoother) due to less nonlinear relationship between the head and the parameters (Yeh et al. 1996).

Drawdown-Based Estimation

For all previous analyses, the true initial conditions were used, and the boundary conditions used to generate the initial condition were also used in the inverse model. In a real world case, aquifer tests are rarely begun from equilibrium and the aquifer's boundary conditions are often poorly known; therefore, a scenario was performed where these were specified incorrectly.

A zero-drawdown specified head boundary condition was specified at all elements around the outside edge of the domain—even for the specified flux and no-flow boundary conditions in the true model (the two bedrock outcrops were still specified as no-flow). At all the observation locations, the drawdown from the pretest condition was used in place of the simulated head. The results from this exercise, shown in Figure 9A and summarized in column 6 in panels a and b of Table 1, indicate that very good results are still obtainable even when the initial or boundary conditions are poorly known. The predicted velocity components (Figure 9B) are not as good as in the case where the initial condition and boundary conditions are perfectly known, but the prediction is still reasonable, indicated by the high ρ_{rank} values.

Discussion

Although a synthetic study can never take into account all the uncertainty potentially present in real world field problems, such as the potential mischaracterization of

a hydrologic system, it can isolate the issues related to data availability and aquifer test design. In this case, we have used the same model type and grid to compute the “true” and inverse solutions; therefore, there is no estimation error due to epistemic uncertainty.

Viability of Other Methods

This work stresses the benefits of using tomographic aquifer tests, and their inversion can be carried out with a variety of different tools. All the results computed here were done using SSLE and the finite-element 2D flow model VSAFT2. Fewer than 10 iterations in SSLE were needed to meet the specified convergence criterion.

Qualitative comparisons of the possible combinations of different “machinery” that could be used to implement the HT inversion outlined here are beyond the scope of this paper, but a similar implementation could be done using public domain software such as MODFLOW (Harbaugh 2005), PEST, or UCODE, which use the perturbation approximation to the sensitivity.

If other methods are used and aquifer properties in each element of the forward model are estimated, then a regularization technique must be employed to reduce the effects of overparameterization. One could effectively increase the number of observations by adding regularization “observations” that the parameter distribution is smooth. Alternatively, one could decrease the number of parameters being estimated. This can be accomplished using a pilot point method (RamaRao et al. 1995), where kriging fills in the model grid with aquifer parameters from a smaller set of estimated values. Another means of accomplishing this is through the singular value decomposition threshold method (Doherty 2007), where only those parameters with large singular values in the estimation process are included. This reduces the dimensionality

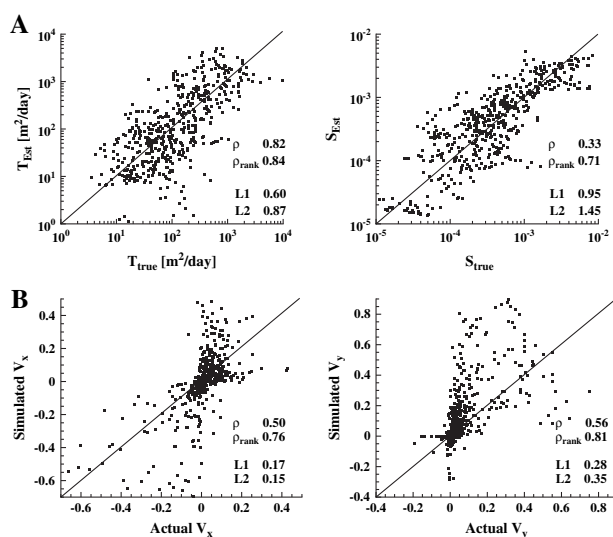


Figure 9. (A) Scatter plots of SSLE-estimated T and S using drawdown and incorrect boundary conditions and (B) scatter plots of x and y components of velocity for SSLE-estimated T and S using drawdown and incorrect boundary conditions.

of the inverse problem without choosing a priori which parameters are more important or where pilot points should be located.

Kalman filters are another class of candidate inversion algorithm; they are popular in control and systems engineering and have been applied hydrologic problems in different ways (Chen and Zhang 2006; Goegebeur and Pauwels 2007). They are more general than nonlinear least squares, since model and measurement noise can be incorporated directly into the inversion process, obviating the need for smoothing noisy data, but they do not have any means of incorporating the spatial correlation between the parameters into the estimation process, as SSLE does.

Conclusions

Based on the numerical experiments performed on the given synthetic regional domain, transient HT inversion using the SSLE is shown to work well for estimating the aquifer parameters T and S on a regional scale. Although all the simulations performed in this work have been done using the SSLE adjoint-based inverse method, this is not the only option.

We address the test scale issue that arises from applying HT to a basin-scale problem by using multiple wells distributed across the basin in each pumping event. We feel this is a realistic way to address the scale problem in a manner that can potentially be applied to monitored municipal or treatment wellfields.

The tomographic approach to analyzing aquifer test data could potentially be used on existing monitoring data. In many basins, there are collections of operational data and numerous aquifer tests that have been conducted through time, which may not provide a great deal of useful basin-wide information individually, but when analyzed together, they can create a whole that is greater than the sum of the parts. Results of this study appear to echo the call by Yeh and Lee (2007): It is time to change the way we collect and analyze data for aquifer characterization.

Acknowledgments

This is an extension of a term project for the advanced subsurface hydrology class (HWR535) offered at the Department of Hydrology and Water Resources at the University of Arizona by the last author; it was partially funded by a Strategic Environmental Research and Development Program (SERDP) grant (ER-1365), sub-contracted through University of Iowa, and National Science Foundation (NSF) IIS-0431079. We would like to thank Michael Fienen and one anonymous reviewer for their detailed and insightful comments.

References

Barlebo, H.C., M.C. Hill, and D. Rosbjerg. 2004. Investigating the Macrodispersion Experiment (MADE) site in Columbus, Mississippi, using a three-dimensional inverse flow and transport model. *Water Resources Research* 40, no. 4: W04211.

Bohling, G.C., J.J. Butler Jr., X. Zhan, and M.D. Knoll. 2007. A field assessment of the value of steady shape hydraulic tomography for characterization of aquifer heterogeneities. *Water Resources Research* 43, no. 5: W05430.

Bohling, G.C., X. Zhan, J.J. Butler Jr., and L. Zheng. 2002. Steady shape analysis of tomographic pumping tests for characterization of aquifer heterogeneities. *Water Resources Research* 38, no. 12: 1324.

Brauchler, R., R. Liedl, and P. Dietrich. 2003. A travel time based hydraulic tomographic approach. *Water Resources Research* 39, no. 12: 1370.

Bredehoeft, J.D. 2003. From models to performance assessment: The conceptualization problem. *Ground Water* 41, no. 5: 571–577.

Chen, Y., and D. Zhang. 2006. Data assimilation for transient flow in geologic formations via ensemble Kalman filter. *Advances in Water Resources* 29, no. 9: 1107–1122.

Doherty, J. 2007. *PEST: Model-independent Parameter Estimation User Manual*, 5th ed. Brisbane, Australia: Watermark Numerical Computing.

Goegebeur, M., and V.R.N. Pauwels. 2007. Improvement of the PEST parameter estimation algorithm through extended Kalman filtering. *Journal of Hydrology* 337, no. 3–4: 436–451.

Gottlieb, J., and P. Dietrich. 1995. Identification of the permeability distribution in soil by hydraulic tomography. *Inverse Problems* 11, no. 2: 353–360.

Hao, Y., T.-C.J. Yeh, J. Xiang, W.A. Illman, K. Ando, and K.-C. Hsu. 2008. Hydraulic tomography for detecting fracture connectivity. *Ground Water* 46, no. 2: 183–192.

Harbaugh, A.W. 2005. The US Geological Survey modular ground-water model, the ground-water flow process. USGS Techniques and Methods 6-A16. Reston, Virginia: USGS.

Hughson, D.L., and T.-C.J. Yeh. 2000. An inverse model for three-dimensional flow in variably saturated porous media. *Water Resources Research* 36, no. 4: 829–839.

Illman, W.A., X. Liu, and A. Craig. 2007. Steady-state hydraulic tomography in a laboratory aquifer with deterministic heterogeneity: Multi-method and multiscale validation of hydraulic conductivity tomograms. *Journal of Hydrology* 341, no. 3–4: 222–244.

Isaaks, E.H., and R.M. Srivastava. 1989. *An Introduction to Applied Geostatistics*. New York: Oxford Press.

Konikow, L.F., and J.D. Bredehoeft. 1992. Groundwater models cannot be validated. *Advances in Water Resources* 15, no. 1: 75–83.

Li, W., A. Englert, O.A. Cirpka, J. Vanderborght, and H. Vereecken. 2007. Two-dimensional characterization of hydraulic heterogeneity by multiple pumping tests. *Water Resources Research* 43, no. 4: W04433.

Liu, S., T.-C.J. Yeh, and R. Gardiner. 2002. Effectiveness of hydraulic tomography: Sandbox experiments. *Water Resources Research* 38, no. 4: WR000338.

Liu, X., W.A. Illman, A.J. Craig, J. Zhu, and T.-C.J. Yeh. 2007. Laboratory sandbox validation of transient hydraulic tomography. *Water Resources Research* 43, no. 5: W05404.

Oreskes, N., K. Shrader-Frechette, and K. Belitz. 1994. Verification, validation and confirmation of numerical models in the earth sciences. *Science* 243, no. 5147: 641–646.

Poeter, E.P., M.C. Hill, E.R. Banta, S. Mehl, and S. Christensen. 2005. UCODE_2005 and six other computer codes for universal sensitivity analysis, calibration, and uncertainty evaluation. USGS Techniques and Methods 6-A11. Reston, Virginia: USGS.

RamaRao, B.S., A.M. LaVenue, G. de Marsily, and M.G. Marietta. 1995. Pilot point methodology for automated calibration of an ensemble of conditionally simulated transmissivity fields, 1, Theory and computational experiments. *Water Resources Research* 31, no. 3: 475–493.

Straface, S., T.-C.J. Yeh, J. Zhu, S. Troisi, and C.H. Lee. 2007. Sequential aquifer tests at a well field, Montalto Uffugo Scalo, Italy. *Water Resources Research* 43, no. 7: W07432.

- Sun, N.-Z., and W.W.-G. Yeh. 1992. A stochastic inverse solution for transient groundwater flow: Parameter identification and reliability analysis. *Water Resources Research* 28, no. 12: 3269–3280.
- Sykes, J.F., J.L. Wilson, and R.W. Andrews. 1985. Sensitivity analysis for steady state groundwater flow using adjoint operators. *Water Resources Research* 21, no. 3: 359–371.
- Tikhonov, A.N., and V.Y. Arsenin. 1977. *Solutions of Ill-Posed Problems*. New York: Halstead Press.
- Tosaka, H., K. Masumoto, and K. Kojima. 1993. Hydropulse tomography for identifying 3-D permeability distribution. In *Proceedings of the Fourth Annual International Conference on High Level Radioactive Waste Management*, 955–959. New York: ASCE.
- Vasco, D.W., H., Keers, and K. Karasaki. 2000. Estimation of reservoir properties using transient pressure data: An asymptotic approach. *Water Resources Research* 36, no. 12: 3447–3465.
- Vesselinov, V.V., S.P. Neuman, and W.A. Illman. 2001. Three-dimensional numerical inversion of pneumatic cross-hole tests in unsaturated fractured tuff: 2. Equivalent parameters, high-resolution stochastic imaging and scale effects. *Water Resources Research* 37, no. 12: 3019–3042.
- Wu, C.-M., T.-C.J. Yeh, J. Zhu, T.H. Lee, N.-S. Hsu, C.-H. Chen, and A. Folch-Sancho. 2005. Traditional analysis of aquifer tests: Comparing apples to oranges? *Water Resources Research* 41, no. 9: W09402.
- Xiang, J. 2007. Stochastic estimation of hydraulic spatial properties. Ph.D. diss., University of Arizona.
- Yeh, T.-C.J. 1992. Stochastic modeling of groundwater flow and solute transport in aquifers. *Journal of Hydrologic Processes* 6, no. 4: 369–395.
- Yeh, T.-C.J., and C.H. Lee. 2007. Time to change the way we collect and analyze data for aquifer characterization. *Ground Water* 45, no. 2: 116–118.
- Yeh, T.-C.J., C.H. Lee, K.-C. Hsu, and Y.-C. Tan. 2007. Fusion of active and passive hydrologic and geophysical tomographic surveys: The future of subsurface characterization. In *Data Integration in Subsurface Hydrology*, ed. D.W. Hyndman, F.D. Day-Lewis, and K. Singha, AGU monograph. Washington, D.C.: American Geophysical Union.
- Yeh, T.-C.J., and S. Liu. 2000. Hydraulic tomography: Development of a new aquifer test method. *Water Resources Research* 36, no. 8: 2095–2105.
- Yeh, T.-C.J., and P.A. Mock. 1996. Structured approach for calibrating steady-state ground-water flow models. *Ground Water* 34, no. 3: 444–450.
- Yeh, T.-C.J., M. Jin, and S. Hanna. 1996. An iterative stochastic inverse method: Conditional effective transmissivity and hydraulic head fields. *Water Resources Research* 32, no. 1: 85–92.
- Yeh, T.-C.J., R. Srivastava, A. Guzman, and T. Harter. 1993. A numerical-model for water-flow and chemical-transport in variably saturated porous-media. *Ground Water* 31, no. 4: 634–644.
- Zhang, J., and T.-C.T.J. Yeh. 1997. An iterative geostatistical inverse method for steady flow in the vadose zone. *Water Resources Research* 33, no. 1: 63–71.
- Zhu, J., and T.-C.T.J. Yeh. 2006. Analysis of hydraulic tomography using temporal moments of drawdown recovery data. *Water Resources Research* 42, no. 2: W02403.
- Zhu, J., and T.-C.T.J. Yeh. 2005. Characterization of aquifer heterogeneity using transient hydraulic tomography. *Water Resources Research* 41, no. 7: W07028.